

Approaches to the sign problem in lattice field theory

Christof Gattringer

*Institut für Physik, Universität Graz,
8010 Graz, Österreich, Austria
christof.gattringer@uni-graz.at*

Kurt Langfeld

*Centre for Mathematical Sciences, Plymouth University,
Plymouth, PL4 8AA, UK
kurt.langfeld@plymouth.ac.uk*

Received 30 March 2016

Accepted 23 May 2016

Published 5 August 2016

Quantum field theories (QFTs) at finite densities of matter generically involve complex actions. Standard Monte Carlo simulations based upon importance sampling, which have been producing quantitative first principle results in particle physics for almost forty years, cannot be applied in this case. Various strategies to overcome this so-called *sign problem* or *complex action problem* were proposed during the last thirty years. We here review the sign problem in lattice field theories, focusing on two more recent methods: dualization to worldline type of representations and the density-of-states approach.

Keywords: Lattice field theory; finite density; dual approach; density of states.

PACS numbers: 11.15.Ha, 12.38.Gc

1. Sign Problem Essentials

Since their infancy, Monte Carlo simulations on space-time lattices have evolved into a powerful quantitative tool for *ab initio* calculations in quantum field theory. However, Monte Carlo methods face major problems when the action S becomes complex and the Boltzmann factor e^{-S} cannot be used as a weight in a stochastic process. Examples for this so-called *sign problem* or *complex action problem* (we use the two terms synonymously) are theories with chemical potential or models with a θ term. Different strategies were explored, and the reviews at the yearly lattice conferences^{1–7} summarize the progress.

After an introduction to the problem, we focus in this short review on two recent strategies for dealing with the complex action problem: the dual approach and

density-of-states techniques. In the dual approach the complex action problem is solved completely by exactly mapping the theory to new variables, the partition sum of which has only real and positive contributions, such that Monte Carlo sampling is feasible. The method is powerful and elegant, but it is not yet clear for which classes of models real and positive dual representations can be found. The density-of-states approach, on the other hand, is a generally applicable strategy, where the challenge is to get under control the numerical accuracy needed for reliable results.

1.1. What is the sign problem?

The aim in finite temperature quantum field theory is to calculate expectation values

$$\langle A \rangle = \frac{1}{Z} \text{Tr}[A \exp(-H/T)], \quad Z = \text{Tr} \exp(-H/T), \quad (1)$$

where H is the Hamiltonian, T the temperature, Z the partition function and A an operator representing an observable. For studying such quantum systems with Monte Carlo methods, they are mapped to a path integral,

$$\begin{aligned} Z &= \sum_{c_1 \dots c_n} \langle c_1 | e^{-aH} | c_2 \rangle \dots \langle c_{n-1} | e^{-aH} | c_1 \rangle \\ &=: \sum_{\{c\}} P(c) \quad (\text{classical representation}). \end{aligned} \quad (2)$$

$P(c)$ is referred to as the *probabilistic weight* of the (classical) *configurations* $c = c_1, \dots, c_n$, and the lattice spacing $a = \frac{1}{nT}$ is the regulator we introduce. Similarly

$$\text{Tr}[A \exp(-H/T)] = \sum_{\{c\}} A(c) P(c). \quad (3)$$

If $P(c)$ is (semi-)positive definite, Monte Carlo simulations generate m configurations c_k , $k = 1, \dots, m$ using *importance sampling* with the weight $P(c)$. Expectation values and the error are estimated by

$$\langle A \rangle \approx \frac{1}{m} \sum_{k=1}^m A(c_k), \quad \text{err}_A \approx \sqrt{\frac{2\tau + 1}{m - 1}} \sigma_A, \quad (4)$$

where τ is the auto-correlation time, and σ_A the standard deviation of the $A(c_k)$.

For studying the grand-canonical ensemble we introduce a chemical potential μ and generalize to $H = H_0 + \mu N$, where N is the particle number operator with $[H, N] = 0$. The key observation is that when repeating the steps to derive the path integral, it generically turns out that, even for bosonic theories, the “weights” $P(c)$ are complex numbers. We illustrate this here for a (one-dimensional) quantum mechanical system, $H_0 = \frac{1}{2} \hat{p}^2 + V(x)$, $N = \hat{p}$, where \hat{p} is the momentum operator.

Using momentum $|p\rangle$ and coordinate $|x\rangle$ eigenstates, we find:

$$\begin{aligned}\langle x_n | e^{-aH} | x_{n+1} \rangle &= \int_{p_n} \langle x_n | e^{-aV(x_n)} | p_n \rangle \langle p_n | x_{n+1} \rangle \exp\left(-\frac{a}{2}p_n^2 - a\mu p_n\right) \\ &= \int_{p_n} e^{-aV(x_n)} e^{-\frac{a}{2}p_n^2 - a\mu p_n} e^{ip_n(x_{n+1}-x_n)} \\ &\propto \exp\left(-\frac{a}{2}\left[\frac{x_{n+1}-x_n}{a} + i\mu\right]^2 - aV(x_n)\right).\end{aligned}\quad (5)$$

In the limit $a \rightarrow 0$, the partition function can be written as an ensemble average over closed “worldlines” parameterized by $x(\tau)$ with $x(0) = x(L)$, $L = 1/T$:

$$Z \propto \int \mathcal{D}x \exp\left(-\int_0^L d\tau \left[\frac{1}{2}(\dot{x} + i\mu)^2 - V(x(\tau))\right]\right). \quad (6)$$

The “string-inspired” representation of quantum systems in terms of worldlines has been used to calculate n -point amplitudes in perturbative quantum field theory (for a review see Ref. 8). The worldline formalism also is a viable numerical tool,⁹ which was applied to study the quantum interaction of vortices¹⁰ or the Casimir effect.¹¹

Here we make two important observations: (i) although Eq. (1) shows that the partition function Z is real and positive, in the form (2) Z only becomes real in the ensemble average, since $P(c)$ in general can be complex. Complex $P(c)$ renders the standard Monte Carlo method impossible since we lose the probability interpretation. (ii) Whether $P(c)$ is real or complex is representation dependent. If we would, e.g. choose the exact eigenstates of the Hamiltonian H , $P(c)$ would be real and positive (note, however, that knowing these eigenstates means that we already solved the problem exactly).

Since the mere existence of the sign problem seems artificial, a proper definition of the problem and of what we would consider a solution is essential. We here follow closely the discussion by Troyer and Wieser:¹²

- A quantum system is defined to suffer from a sign problem if there occur negative (or complex) weights $P(c)$ in the classical representation.
- An algorithm for the stochastic estimate of an expectation value such as $\langle A \rangle$ is of *polynomial complexity* if the computational time $t(\epsilon, V, T)$ needed to achieve a relative statistical error $\epsilon = \text{err}_A / \langle A \rangle$ scales polynomial with the system size V , i.e. there exist integers n and ν (and a finite constant κ) such that $t(\epsilon, V, T) < \kappa \epsilon^{-2} \frac{V^n}{T^\nu}$.
- For a quantum system suffering from a sign problem for A , for which there exists a polynomial complexity algorithm for a related classical system, we call this algorithm a *solution of the sign problem* for the calculation of $\langle A \rangle$.

1.2. Why does the reweighting algorithm not solve sign problems?

In the eighties *reweighting* was proposed for quantum systems where the weight $P(c)$ of the corresponding classical formulation is complex (or not strictly positive):

$$P(c) = \exp(i\varphi(c))|P(c)|, \quad \varphi(c) \neq 0 \quad \text{for some } c. \quad (7)$$

If Monte Carlo configurations c' are generated with respect to $|P(c)|$, the expectation value in (1) can formally be written in terms of estimators with respect to configurations c' : $\langle A \rangle = \langle A(c') \exp(i\varphi(c')) \rangle_R / \langle \exp(i\varphi(c')) \rangle_R$. The key observation is that the expectation values $\langle \cdots \rangle_R$ *cannot* be estimated in polynomial time for a given relative error ϵ . Hence, the reweighting algorithm fails one of the criteria for qualifying as solution. We illustrate this for the phase factor expectation value. Following Ref. 12, we write this expectation value as ratio of two partition functions,

$$\langle \exp(i\varphi(c')) \rangle_R = \frac{Z}{Z'}, \quad Z = \sum_c p(c), \quad Z' = \sum_c |p(c)|. \quad (8)$$

The quantum systems related to Z and Z' possess different free energy densities, denoted as f and f' . Hence, we find

$$\langle \exp(i\varphi(c')) \rangle_R = \exp\left(-\frac{\Delta f}{T} V\right), \quad \Delta f \equiv f - f'. \quad (9)$$

The triangle inequality implies $\langle \exp(i\varphi(c')) \rangle_R \leq 1$, giving rise to $\Delta f \geq 0$. Thus, we find that $Q := \langle \exp(i\varphi) \rangle$ is exponentially suppressed with the volume. In an actual Monte Carlo simulation, a significant portion of the configurations produce contributions $\exp(i\varphi(c'))$ of order 1. Hence, the error for the phase factor is only suppressed by the Monte Carlo “run-time” m leaving us with

$$\text{err}_Q = \frac{\sigma}{\sqrt{m}}, \quad \frac{\text{err}_Q}{Q} = \frac{\sigma}{\sqrt{m}} \exp\left(\frac{\Delta f}{T} V\right). \quad (10)$$

As expected, the reweighting is *not* of polynomial complexity.

In the remainder of this paper, we focus on two methods that bear the potential to be of polynomial complexity. (i) The exact reformulation of a model to a dual formulation in terms of new variables such that all $P(c)$ are real and positive (see Sec. 2). Moreover, the dual version quite often allows for very efficient simulations using flux or worm algorithms. (ii) The complexity of the so-called density-of-states method (see Sec. 3) is not yet clear: however, this approach is not entirely stochastic — it has an element of direct integration, and secondly, the method features an exponential error suppression, which might help to counterbalance any difference in the free energy densities such as in (10).

2. Dualization and Flux Simulations

As already mentioned, the dual approach consists of a mapping of the theory to new variables (dual variables) such that the partition sum has only real and positive contributions. Monte Carlo sampling then is possible in terms of the dual variables.

The dual variables approach is powerful and elegant, but it is *a priori* unclear for which class of theories a real and positive dual representation is possible.

However, some of the structure of the dual variables is well understood by now and the toolbox for dual mappings is growing continuously. In general one trades the conventional representation in terms of classical fields in a path integral for new integer valued variables which, however, are subject to constraints such that they give rise to a geometrical interpretation in terms of worldlines and worldsheets.

The dual variables for matter can be viewed as closed loops on the links of the lattice. The flux along the loops is unbounded for bosons, while it can only be 0 or 1 for each element of fermion flux. The dual variables for gauge fields are surfaces, which either are closed surfaces or surfaces bounded by matter flux. Alternatively, the surfaces can be viewed as being built from cycles of flux around elementary plaquettes, and again the flux around these cycles can be from all integers. We stress at this point that the dual representation of a lattice field theory is not unique. For some systems, several different dual representations are known and it is an interesting open question how these are related and how the underlying symmetries of a theory in the conventional representation manifest themselves in the dual form.

In this section of our review, we discuss dual variables by first presenting the general idea of the dual approach for a simple charged scalar field (relativistic Bose gas). Subsequently, we discuss the generalization to systems with Abelian gauge fields and conclude the presentation of the dual approach with addressing open challenges.

2.1. A prototype example: The dual form of a charged scalar field

A theory which is well suited for presenting the idea of the dual approach is the charged scalar field which is described by the lattice action

$$S = \sum_x \left(\eta |\phi_x|^2 + \lambda |\phi_x|^4 - \sum_{\nu=1}^4 \left[e^{\mu \delta_{\nu,4}} \phi_x^* \phi_{x+\hat{\nu}} + e^{-\mu \delta_{\nu,4}} \phi_x^* \phi_{x-\hat{\nu}} \right] \right). \quad (11)$$

The conventional degrees of freedom are the complex valued fields $\phi_x \in \mathbb{C}$ on the sites x of a four-dimensional lattice with periodic boundary conditions. We use $\eta = m^2 + 8$, where m is the mass of the field. By λ we denote the quartic coupling and μ is the chemical potential, which gives a different weight to forward and backward hopping in time direction ($\nu = 4$). It is obvious that for finite μ , the action has a nonvanishing imaginary part and in the conventional representation the model has a complex action problem. The partition sum $Z = \int D[\phi] e^{-S}$ is obtained by integrating the Boltzmann factor e^{-S} with the product measure $\int D[\phi] = \prod_x \int_{\mathbb{C}} \frac{d\phi_x}{2\pi}$.

To obtain the dual representation, we follow Refs. 13 and 14: the contribution from the nearest neighbor terms of (11) to the Boltzmann factor is written

as the product

$$\begin{aligned}
 & \prod_{x,\nu} \exp(e^{\mu\delta_{\nu,4}} \phi_x^* \phi_{x+\hat{\nu}}) \exp(e^{-\mu\delta_{\nu,4}} \phi_x \phi_{x+\hat{\nu}}^*) \\
 &= \sum_{\{n,\bar{n}\}} \left(\prod_{x,\nu} \frac{1}{n_{x,\nu}! \bar{n}_{x,\nu}!} \right) \left(\prod_x e^{\mu[n_{x,4} - \bar{n}_{x,4}]} \right) \left(\prod_{x,\nu} (\phi_x^* \phi_{x+\hat{\nu}})^{n_{x,\nu}} (\phi_x \phi_{x+\hat{\nu}}^*)^{\bar{n}_{x,\nu}} \right) \\
 &= \sum_{\{n,\bar{n}\}} \left(\prod_{x,\nu} \frac{1}{n_{x,\nu}! \bar{n}_{x,\nu}!} \right) \left(\prod_x e^{\mu[n_{x,4} - \bar{n}_{x,4}]} \phi_x^* \sum_{\nu} [n_{x,\nu} + \bar{n}_{x-\hat{\nu},\nu}] \phi_x \sum_{\nu} [\bar{n}_{x,\nu} + n_{x-\hat{\nu},\nu}] \right), \quad (12)
 \end{aligned}$$

where in the second step we expanded the individual exponentials and subsequently reorganized the terms in the product. We use the abbreviation $\sum_{\{n,\bar{n}\}} = \prod_{x,\nu} \sum_{n_{x,\nu}=0}^{\infty} \sum_{\bar{n}_{x,\nu}=0}^{\infty}$ for denoting the sum over all configurations of the expansion indices $n_{x,\nu}, \bar{n}_{x,\nu} \in \mathbb{N}_0$. In the form (12), one can now integrate the contribution from the nearest neighbor terms with the on-site measures $\prod_x \int_{\mathbb{C}} \frac{d\phi_x}{2\pi} e^{-\eta|\phi_x|^2 - \lambda|\phi_x|^4}$.

An important step in the dualization is to separate the degrees of freedom (dof.) which reflect the symmetry of the theory from all other dof., since integrating out the dof. related to symmetries will generate the constraints for the dual variables. For our example, the symmetry is a global $U(1)$ rotation of the fields, $\phi_x \rightarrow e^{i\alpha} \phi_x$ which leaves the action (11) and the measure $\int D[\phi]$ invariant. For the terms that remain in the effective measure $\prod_x \int_{\mathbb{C}} \frac{d\phi_x}{2\pi} e^{-\eta|\phi_x|^2 - \lambda|\phi_x|^4}$ this is even a local symmetry. To separate the symmetry from the radial dofs. we write the field variables in polar coordinates $\phi_x = r_x e^{i\theta_x}$, and obtain for the partition sum

$$\begin{aligned}
 Z &= \sum_{\{n,\bar{n}\}} \left(\prod_{x,\nu} \frac{1}{n_{x,\nu}! \bar{n}_{x,\nu}!} \right) \left(\prod_x \int_{-\pi}^{\pi} \frac{d\theta_x}{2\pi} e^{-i\theta_x \sum_{\nu} [n_{x,\nu} - \bar{n}_{x,\nu} - (n_{x-\hat{\nu},\nu} - \bar{n}_{x-\hat{\nu},\nu})]} \right) \\
 &\quad \times \left(\prod_x e^{\mu[n_{x,4} - \bar{n}_{x,4}]} \int_0^{\infty} dr_x r_x^{1 + \sum_{\nu} [n_{x,\nu} + n_{x-\hat{\nu},\nu} + \bar{n}_{x,\nu} + \bar{n}_{x-\hat{\nu},\nu}]} e^{-\eta r_x^2 - \lambda r_x^4} \right). \quad (13)
 \end{aligned}$$

The integrals over the phases give rise to Kronecker deltas, which implement the constraints. To make more evident the flux nature of the dual variables, we finalize the dualization by a change of the discrete variables and switch to new variables $k_{x,\nu} \in \mathbb{Z}$ and $l_{x,\nu} \in \mathbb{N}_0$, which are related to $n_{x,\nu}, \bar{n}_{x,\nu}$ by

$$n_{x,\nu} - \bar{n}_{x,\nu} = k_{x,\nu} \quad \text{and} \quad n_{x,\nu} + \bar{n}_{x,\nu} = |k_{x,\nu}| + 2l_{x,\nu}, \quad (14)$$

and constitute the set of dual variables used in the final form of the partition sum

$$Z = \sum_{\{k,l\}} \left(\prod_{x,\nu} \frac{1}{(|k_{x,\nu}| + l_{x,\nu})! l_{x,\nu}!} \right) \left(\prod_x W(s_x) \right) e^{\mu \sum_x k_{x,4}} \prod_x \delta(\nabla_{\nu} k_{x,\nu}), \quad (15)$$

where $W(n) = \int_0^{\infty} dr e^{-\eta r^2 - \lambda r^4} r^{n+1}$, $s_x = \sum_{\nu} [|k_{x,\nu}| + |k_{x-\hat{\nu},\nu}| + 2(l_{x,\nu} + l_{x-\hat{\nu},\nu})]$, and we denote the discrete divergence as $\nabla_{\nu} k_{x,\nu} = \sum_{\nu} [k_{x,\nu} - k_{x-\hat{\nu},\nu}]$. For a numerical simulation, the $W(n)$ can easily be precomputed numerically and stored.

In the final form (15), the partition function is written as a sum over all configurations of the dual variables $k_{x,\nu} \in \mathbb{Z}$ and $l_{x,\nu} \in \mathbb{N}_0$. The dual variables $k_{x,\nu}$ are subject to constraints which were generated when integrating out the phases θ_x , which correspond to the global $U(1)$ symmetry of the original theory and even a local symmetry of the on-site measure $\prod_x \int_{\mathbb{C}} \frac{d\phi_x}{2\pi} e^{-\eta|\phi_x|^2 - \lambda|\phi_x|^4}$. The constraints $\nabla_\nu k_{x,\nu} = 0, \forall x$ imply vanishing divergence for $k_{x,\nu}$, i.e. the $k_{x,\nu}$ have the interpretation of conserved flux. The dual variables $l_{x,\nu}$ are not subject to constraints and via s_x enter in the weight factors $W(s_x)$ from integrating the radial degrees of freedom. It is obvious that also for finite μ , the dual partition sum (15) has only real and positive contributions and the complex action problem is solved completely.

In the dual form the particle number has a beautiful geometrical interpretation: We already noted that the discrete flux $k_{x,\nu}$ is constrained to vanishing divergence $\nabla_\nu k_{x,\nu} = 0$, and the admissible configurations of $k_{x,\nu}$ are closed flux lines. This gives rise to a simple interpretation of the particle number \mathcal{N} which in the grand canonical ensemble couples in the form $e^{\mu\beta\mathcal{N}}$, where β is the inverse temperature. In the dual representation, μ couples to $\sum_x k_{x,4}$, i.e. the total flux in time direction (= the 4-direction). Since the k -flux is conserved this sum equals to $N_t w[k]$, where N_t is the temporal extent of the lattice and $w[k]$ is the winding number of the flux around the compact time direction. Since in lattice units $\beta = N_t$, we identify $\mathcal{N} = w[k]$, i.e. the particle number is given by the temporal winding number of the flux.

So far we only discussed the transformation of the partition sum to the dual representation. However, for addressing physical questions we also need to identify observables in terms of the dual variables. The simplest way to obtain vacuum expectation values of observables is by derivatives of $\ln Z$ with respect to the couplings of the theory. A derivative with respect to $\mu\beta$ will give rise to the expectation value $\langle \mathcal{N} \rangle$, where in the dual representation the particle number \mathcal{N} is given by the winding number $w[k]$ of k -flux as discussed above. A derivative with respect to η will give rise to the expectation value $\langle \sum_x |\phi_x|^2 \rangle$, which in the dual representation is a sum of ratios of weight factors, $|\phi_x|^2 \sim \sum_x W(s_x + 2)/W(s_x)$. In a similar way also the corresponding susceptibilities can be expressed by sums of dual weights.

More generally, one can also make the couplings depend on the lattice point and take derivatives with respect to these local couplings to generate n -point functions. The dualization goes through without major changes and after taking the respective derivatives all local couplings are set to the desired global value. The n -point functions are then expressed in terms of correlators of the dual variables. In some cases, an even more general approach is possible, where a more general dualization in the presence of source terms can be found. These source terms typically give rise to a larger space of dual variables, e.g. by introducing new dual elements such as open strings with endpoints. Again one can take derivatives with respect to the sources also in the dual form of the partition sum and finds a representation of the observables in the enlarged dual space (see, e.g. Refs. 14, 15 and 16).

An important challenge is how to efficiently update the dual systems. We have seen that the dual variables are subject to constraints, which give rise to the interpretation of closed loops of flux. Consequently, for a Monte Carlo update, the trial configurations one proposes also have to obey the constraints. For bosonic theories local changes, such as changing the loop along a plaquette combined with proposing globally winding loops are an option, however, usually are rather inefficient. An elegant and often very efficient approach is the Prokof'ev–Svistunov worm algorithm.¹⁷ Here, one violates the constraints at a site of the lattice and subsequently propagates the defect along links of the lattice thus creating the “worm”. Each step of the worm is accepted with a Metropolis decision based on the local changes of the weight. The update is concluded once the head of the worm reaches the starting point and all violated constraints are healed. Various generalizations of the worm algorithm were discussed in the context of lattice field theories — see, e.g. Refs. 15, 18–20 and several of the papers cited below.

With dualization techniques similar to those discussed for our example of the scalar field, successful, i.e. real and positive dual mappings were obtained for several scalar field theories: The $O(2)$ model with chemical potential,²¹ various variants of ϕ^4 theories,^{13,14,22–25} $O(N)$ models,^{26–31} $CP(N-1)$ models^{29,32} and the $SU(2)$ chiral model.³³ An interesting line of work are the papers by the Berlin group, where high precision dual simulations were used to revisit the problem of triviality of ϕ^4 theory.^{22–25} Among the systems relevant for particle physics are also spin systems with a chemical potential which serve as effective theories for finite density QCD.^{34–40} Also, for some of these models, successful dualizations based on similar techniques as discussed above were presented in recent years.^{19,20,41,42}

2.2. Theories with gauge fields

Let us now switch from scalar field theories to the more involved case of Abelian gauge theories and Abelian gauge-Higgs theories.^a For the case of $U(1)$ gauge fields, the dualization with a strategy similar to the one used in the last section is straightforward (we here follow the presentation in Ref. 43). The dynamical degrees of freedom are the link variables $U_{x,\mu} \in \mathbb{C}$ living on the links of the lattice. The action is given by $S = -\beta \sum_x \sum_{\mu < \nu} \text{Re} (U_{x,\mu} U_{x+\hat{\mu},\nu} U_{x+\hat{\nu},\mu}^* U_{x,\nu}^*)$, such that we find for the partition sum of pure $U(1)$ lattice gauge theory

$$Z = \int D[U] e^{-S} = \int D[U] \prod_x \prod_{\mu < \nu} e^{\frac{\beta}{2} [U_{x,\mu} U_{x+\hat{\mu},\nu} U_{x+\hat{\nu},\mu}^* U_{x,\nu}^* + U_{x,\mu}^* U_{x+\hat{\mu},\nu}^* U_{x+\hat{\nu},\mu} U_{x,\nu}]}, \quad (16)$$

where the path integral measure is given by $\int D[U] = \prod_{x,\mu} \int_{U(1)} dU_{x,\mu}$.

For the case of $U(1)$ gauge theory, where the contributions to the action are pure phases, we can simplify the dualization by using the fact that each term in

^aSo far real and positive dual representations were found only for Abelian gauge fields.

the Boltzmann factor has the form of the generating functional for modified Bessel functions I_n given by $e^{\frac{z}{2}[t+t^{-1}]} = \sum_{n \in \mathbb{Z}} I_n(z) t^n$ where $z, t \in \mathbb{C}, t \neq 0$. We introduce integer valued variables $p_{x,\mu,\nu} \in \mathbb{Z}$ and expand each exponent in (16) using the generating functional and find

$$\begin{aligned} Z &= \int D[U] \prod_x \prod_{\mu < \nu} \sum_{p_{x,\mu,\nu} \in \mathbb{Z}} I_{p_{x,\mu,\nu}}(\beta) (U_{x,\mu} U_{x+\hat{\mu},\nu} U_{x+\hat{\nu},\mu}^* U_{x,\nu}^*)^{p_{x,\mu,\nu}} \\ &= \sum_{\{p\}} \prod_{x,\mu < \nu} I_{p_{x,\mu,\nu}}(\beta) \prod_{x,\mu < \nu} \int_{U(1)} dU_{x,\mu} (U_{x,\mu})^{-F_{x,\mu}[p]} \\ &= \sum_{\{p\}} \prod_{x,\mu < \nu} I_{p_{x,\mu,\nu}}(\beta) \prod_{x,\mu} \delta(F_{x,\mu}[p]), \end{aligned} \quad (17)$$

with $F_{x,\mu}[p] = \sum_{\rho: \rho < \mu} [p_{x,\rho,\mu} - p_{x-\hat{\rho},\rho,\mu}] - \sum_{\nu: \mu < \nu} [p_{x,\mu,\nu} - p_{x-\hat{\nu},\mu,\nu}]$. In the second step of (17), we have reorganized the powers of the $U_{x,\mu}$ and $U_{x,\mu}^* = U_{x,\mu}^{-1}$, thus collecting the exponents $F_{x,\mu}[p]$, and introduced the sum $\sum_{\{p\}}$ over all configurations of the $p_{x,\mu,\nu}$. In the last step, we have used $\int_{U(1)} dU U^n = \delta(n)$, where $\delta(n)$ denotes the Kronecker delta. Obviously the dualization has only real and positive terms. Here, the constraints are based on the links of the lattice and require that the combination $F_{x,\mu}[p]$ vanishes at each link.

Again, we have an interesting geometrical interpretation of the dual form of the theory: The plaquette occupation numbers $p_{x,\mu,\nu}$ may be viewed as occupation numbers for flux around the contours of the plaquette (x, μ, ν) , where positive (negative) $p_{x,\mu,\nu}$ is for mathematically positive (negative) orientation. The combination $F_{x,\mu}[p]$ thus is the total flux from all plaquettes that contain the link (x, μ) . The constraint simply implements vanishing total flux at each link of the lattice. If one now for example considers a configuration with only plaquette occupation numbers $p_{x,\mu,\nu} = -1, 0$ or $+1$, then the constraints imply that the occupied plaquettes form closed, oriented surfaces. Since plaquette occupation numbers can simply be added, a general configuration with arbitrary $p_{x,\mu,\nu}$ can be viewed as a superposition of such closed surfaces. Thus, the partition sum (17) can also be interpreted as a sum over closed surfaces. The weights $I_{p_{x,\mu,\nu}}(\beta)$ then simply take into account the net number $p_{x,\mu,\nu}$ of how often a plaquette (x, μ, ν) appears in the configuration of surfaces. As for the relativistic Bose gas discussed above, we can obtain the relevant observables, i.e. the action density and the corresponding susceptibility by derivatives with respect to β . Studies of Abelian gauge theories in the dual formulation can be found in various variants (see Refs. 27, 44–48 for a selection).

In two dimensions, the mapping of $U(1)$ gauge theory can easily be generalized by including a topological term, i.e. the addition of $i\theta Q$ to the action, where $Q = \frac{1}{2\pi} \int d^2x \epsilon_{\mu\nu} F_{\mu\nu}(x)$ is the topological charge. In the conventional representation, this

system now has a complex action problem for $\theta \neq 0$. A simple discretization of the $U(1)$ topological charge in 2 dimensions is $i\theta Q = \frac{\theta}{2\pi} \sum_x \text{Im} U_{x,1} U_{x+\hat{1},2} U_{x+\hat{2},1}^* U_{x,2}^*$. Using this so-called field theoretical discretization, the combined Boltzmann factor from action and topological charge reads for a single plaquette

$$e^{\eta U_x + \bar{\eta} U_x^*} = \sum_{p_x \in \mathbb{Z}} I_{|p_x|}(2\sqrt{\eta\bar{\eta}}) \left(\sqrt{\frac{\eta}{\bar{\eta}}} \right)^{p_x} U_x^{p_x}, \quad (18)$$

where $U_x = U_{x,1} U_{x+\hat{1},2} U_{x+\hat{2},1}^* U_{x,2}^*$ and $\eta = \frac{\beta}{2} - \frac{\theta}{4\pi}$, $\bar{\eta} = \frac{\beta}{2} + \frac{\theta}{4\pi}$. In the second step, we have already used an expansion formula (see, e.g. Ref. 49 for a derivation), which generalizes the generating functional for the Bessel functions. Proceeding as before, one obtains the dualization of 2-d $U(1)$ lattice gauge theory with a topological term,

$$Z = \sum_{\{p\}} \prod_x I_{|p_x|}(2\sqrt{\eta\bar{\eta}}) \left(\sqrt{\frac{\eta}{\bar{\eta}}} \right)^{p_x} \delta(p_x - p_{x-\hat{2}}) \delta(p_{x-\hat{1}} - p_x). \quad (19)$$

Again the partition sum is a sum over all configurations of the integer valued plaquette occupation number $p_x \in \mathbb{Z}$ subject to the constraints implemented by the Kronecker deltas in (19). Also for nonzero θ , the partition sum has only real and positive contributions, and (19) is the first successful real and positive dualization for a theory with a vacuum angle (compare Refs. 50 and 51 for some numerical results).

The generalization of the dualization of Abelian gauge theories together with the dualization of the scalar field theory discussed in the previous subsection to a dualization of Abelian gauge-Higgs models is rather straightforward. When gauge fields are coupled to the action of the charged scalar given in (11), then the nearest neighbor terms are made gauge invariant by multiplying them with the gauge links $U_{x,\mu} \in U(1)$. The dual mapping as discussed in Subsec. 2.1 goes through essentially unchanged. The only modification is that now the loops that appear in the dual partition sum (15) are dressed with link variables. These link variables are integrated over with the gauge action, which is again expanded as in (17). Thus, the dual variables $k_{x,\nu}$ alter the constraints for the plaquette occupation numbers $p_{x,\mu,\nu}$. As a consequence in the gauge-Higgs model, the surfaces can have boundaries and the link-constraints along the boundaries are saturated by matter flux $k_{x,\nu}$.

We here give the final result for the dual representation of the $U(1)$ gauge-Higgs model with two flavors of opposite charge. This is an interesting case because in this electrically neutral system, finite density of charges is possible, i.e. a chemical potential can be coupled in a meaningful way. The fields corresponding to the two charges can have different masses m and \bar{m} , different couplings λ and $\bar{\lambda}$, as well as different chemical potentials μ and $\bar{\mu}$. For the two-flavor case, we have two sets of dual variables for the matter field, the $k_{x,\nu} \in \mathbb{Z}$, $l_{x,\nu} \in \mathbb{N}_0$ of (17) and another set $\bar{k}_{x,\nu} \in \mathbb{Z}$, $\bar{l}_{x,\nu} \in \mathbb{N}_0$ for the second flavor. The dual partition function is a sum over

the configurations of all variables $k_{x,\nu}$, $l_{x,\nu}$, $\bar{k}_{x,\nu}$, $\bar{l}_{x,\nu}$, $p_{x,\mu,\nu}$,

$$\begin{aligned}
 Z = & \sum_{\{k,l,\bar{k},\bar{l},p\}} \prod_{x,\nu} \frac{1}{(|k_{x,\nu}| + l_{x,\nu})! l_{x,\nu}!} \frac{1}{(|\bar{k}_{x,\nu}| + \bar{l}_{x,\nu})! \bar{l}_{x,\nu}!} \\
 & \times \prod_x W(s_x) \bar{W}(\bar{s}_x) \prod_x \prod_{\mu < \nu} I_{p_{x,\mu,\nu}}(\beta) e^{\mu \sum_x k_{x,4}} e^{\bar{\mu} \sum_x \bar{k}_{x,4}} \\
 & \times \prod_x \delta(\nabla_\nu k_{x,\nu}) \delta(\nabla_\nu \bar{k}_{x,\nu}) \prod_x \prod_\nu \delta(F_{x,\nu}[p] - k_{x,\nu} + \bar{k}_{x,\nu}). \quad (20)
 \end{aligned}$$

All conventions for s_x and $W(s_x)$ are taken over from (15) with \bar{s}_x computed from the dual variables $\bar{k}_{x,\nu}$, $\bar{l}_{x,\nu}$ and $\bar{W}(\bar{s}_x)$ using \bar{m} , $\bar{\lambda}$. As in the case of the charged scalar field also here the complex action problem is solved completely, since the chemical potentials μ and $\bar{\mu}$ appear again as coupling to the temporal winding number of k and \bar{k} flux in the real and positive exponential form.

Dual representations for U(1) gauge-Higgs models with chemical potential were simulated in Refs. 43 and 52, mainly with the motivation of studying condensation phenomena at finite μ ; the structurally similar case of the \mathbb{Z}_3 gauge-Higgs system was analyzed, too.⁵³ Also in two dimensions U(1) gauge-Higgs systems are of interest, since with the topological angle θ one has an additional parameter to probe the physics of the system.^{50,51} Concerning the update of the gauge degrees of freedom different options were explored.^{27,45,54} For the more general case of gauge-Higgs systems, the fact that the link-constraints of the plaquettes can also be saturated with matter flux allows for an interesting generalization of the Prokof'ev–Svistunov worm algorithm:¹⁷ After placing a unit of matter flux on a randomly chosen link one adds plaquettes with occupation numbers ± 1 where for two of the links of the plaquette the constraints are satisfied by matter flux. In this way, one transports the defects on a link and its endpoints across the lattice in the same way as the usual worm transports a defect located on sites. Every step of this so-called surface-worm algorithm (SWA)⁵⁴ is governed by a random decision and a Metropolis acceptance step and the SWA was shown to update Abelian gauge-Higgs systems very efficiently.

2.3. Future challenges for the dual approach

Let us now come to a short discussion of the main open challenges for the dual approach: non-Abelian gauge fields and fermions. Here, often dualities were studied only in certain limits, in particular for strong coupling and large fermion mass.

The successful dualization we have discussed for the U(1) case is based on expanding the gauge field Boltzmann factor in $\beta = 1/e^2$, i.e. it is a strong coupling expansion. Thus, also for other gauge groups approaches based on the strong coupling expansion can be found in the literature^{55–67} and in some of the works cited below. Several of these papers include only (very) few terms of the strong coupling expansion, while some attempt a complete formal treatment based on the character expansion, which, however, has manifestly negative weight factors

already for pure gauge theories such that a sign problem is actually introduced by the dualization. It is probably fair to conclude that so far no convincing approach for dualizing non-Abelian gauge fields has emerged.

For fermions, the Grassmann nature of the variables in the path integral introduces additional challenges. One can proceed similarly to the charged boson field in Subsec. 2.1 and expand the individual Boltzmann factors for the link and on-site terms. At first glance, this looks even simpler than the bosonic case, since the series terminate after the linear term due to the nilpotency of the Grassmann variables, thus allowing only fluxes (or “occupation numbers”) 0 and 1. However, for the subsequent integration, the Grassmann variables must be brought into their canonical order and the necessary commutations introduce signs for the loops. In addition, also the γ -matrices (or staggered sign factors) introduce signs and phases. Thus, in general, one is left with signs for matter loops summed over in the partition function. Another approach to obtain a loop representation is hopping expansion where with the help of the trace-log formula the fermion determinant is written as exponential of a sum of loops. This exponential can be expanded, giving a loop representation for the fermionic partition sum, which is integrated over the gauge fields. However, also here signs from the fermionic character and the γ -matrices remain.

A simple way to get rid of the signs is to consider $U(1)$ gauge fields in the strong coupling limit, which reduces the theory to a loop model of mesons, i.e. a bosonic loop model without signs (see, e.g. Refs. 68–70). Also for other gauge groups, loop models were derived in the strong coupling limit and interesting numerical results could be obtained, partly by treating the fermions in the large mass limit by including only leading (sometimes resummed) terms in the hopping expansion.^{39,55,56,65–67,71,72}

An area with quite some progress are $(1+1)$ -dimensional theories with fermions. There the topology of the loops is simpler and both the signs from the staggered formulation, as well as the signs from the traces over the γ -matrices of the Wilson formulation can be computed in closed form.⁷³ As a result, one finds that the massless Schwinger model with staggered fermions has a real and positive loop representation in the presence of both, a chemical potential or a vacuum term.⁴⁹ This result can be generalized to a real and positive dual model for a system of one-dimensional nanowires interacting with the four-dimensional electromagnetic field.⁷⁴ For full QED in four dimensions a positive dualization was presented for a subset of the fermion loops, so-called quasi-planar loops, in Ref. 75. It is interesting to note that for the massive Schwinger model (except at strong coupling) the signs come back.⁷⁶ Finally, also for two-dimensional models with 4-Fermi interaction, several successful dual formulations can be found in the literature.^{77–81}

An interesting idea related to some of the techniques presented here is the fermion bag approach.⁸² There the action is split into a free fermion part and a fermion self-interaction. For the interaction part, the local Boltzmann factors are expanded and if the corresponding term is activated, it locally saturates the

Grassmann integrals. On the remaining sites, the “fermion bags,” one propagates free fermions with standard methods. The approach was shown to be very efficient for several models and interesting physics results were obtained.^{83–85}

Let us conclude the section about dual methods with a speculation: With the growing number of successfully dualized models, we begin to understand how different symmetries of the conventional formulation manifest themselves in terms of dual variables. A deeper understanding of symmetries and dual variables might eventually lead to the possibility of model building directly in terms of dual variables. Although many open questions need to be answered, such as under which modifications of the dual representation does the universality class remain the same, and how are different known dualizations of the same model related to each other, the idea of formulating models directly in terms of dual variables is an exciting perspective for quantum field theories on the lattice.

3. The Density-of-States Approach

3.1. The method

Although the density-of-states (DoS) approach involves a Monte Carlo element in one way or another, it does not fall into the class of Markov chain Monte Carlo simulations. While the DoS ρ enumerates the amount of configurations for a given action hypersurface in configuration space, the partition function is recovered by performing one-dimensional numerical integrals:

$$\rho(E) = \int \mathcal{D}\phi \delta(S[\phi] - E), \quad Z(\beta) = \int \mathcal{D}\phi e^{\beta S[\phi]} = \int dE \rho(E) e^{\beta E}. \quad (21)$$

By contrast, conventional Monte Carlo calculations based on importance sampling generate the configurations contributing to the integral with probability

$$P_\beta(E) = \rho(E) e^{\beta E} / Z(\beta).$$

In this standard approach, so-called *overlap* problems occur if an observable strongly depends on configurations in an action range that has low probability according to importance sampling. Key to the success of DoS techniques is that $\rho(E)$ can be calculated with good relative precision over the action range of interest. The overlap problem in this case is avoided by a direct integration of (21). Wang and Landau⁸⁶ provided an efficient algorithm, based upon histograms, for accessing the density of states in a statistical system with a discrete spectrum. For systems with continuous spectrum, however, the histogram based method breaks down even on systems of moderate size.^{87,88} More sophisticated techniques, as for instance those proposed by Berg and Neuhaus,⁸⁹ alleviate the problem by using the Wang–Landau method to compute the weights for a multi-canonical recursion.

Here, we will focus on a novel and promising new method, which falls into the class of Wang–Landau-type approaches and which is called the Logarithmic Linear Relaxation (LLR) algorithm.⁹⁰ Rather than using histograms to estimate the slope

of the DoS, the method avoids uncertainties from histogram edge effects and instead employs expectation values and a stochastic nonlinear equation for this task:

$$\langle\langle W[\phi] \rangle\rangle_k(a) = \frac{1}{\mathcal{N}_k} \int \mathcal{D}\phi \theta_{[E_k, \delta E]}(S[\phi]) W[\phi] e^{-aS[\phi]}, \quad (22)$$

$$\mathcal{N}_k = \int \mathcal{D}\phi \theta_{[E_k, \delta E]} e^{-aS[\phi]} = \int_{E_k}^{E_k + \delta E} dE \rho(E) e^{-aE}, \quad (23)$$

where we have used (21) to express \mathcal{N}_k as an ordinary integral. We also introduced the modified Heaviside function

$$\theta_{[E_k, \delta E]}(S) = \begin{cases} 1 & \text{for } E_k \leq S \leq E_k + \delta E, \\ 0 & \text{otherwise.} \end{cases}$$

Note that $\langle\langle W[\phi] \rangle\rangle_k$ can be estimated by standard Monte Carlo techniques. Let us now specialize to the particular observable $W[\phi] = \Delta E = S[\phi] - E_k - \delta E/2$, the expectation value of which can be written as an integral using again (21):

$$\langle\langle \Delta E \rangle\rangle_k(a) = \frac{1}{\mathcal{N}_k} \int_{E_k}^{E_k + \delta E} dE \rho(E) \left[E - E_k - \frac{\delta E}{2} \right] e^{-aE}. \quad (24)$$

At the heart of the LLR algorithm is the stochastic nonlinear equation for determining the parameter a :⁹⁰

$$\langle\langle \Delta E \rangle\rangle_k(a) = 0 \Leftrightarrow a = \left. \frac{d \ln \rho}{dE} \right|_{E=E_k + \frac{\delta E}{2}} + \mathcal{O}(\delta E^2). \quad (25)$$

It was shown⁹¹ that for sufficiently small δE , there is only one solution to (25). The solution $a = a_k$ of the stochastic equation (25) provides the log-derivative of the density-of-states at the midpoint of the action interval. Finding the solution starts with a standard Newton–Raphson iteration, which departs from an initial guess $a^{(0)}$ and produces a sequence $a^{(0)} \rightarrow a^{(1)} \rightarrow \dots \rightarrow a^{(n)} \rightarrow a^{(n+1)} \dots$ using

$$a^{(n+1)} = a^{(n)} + \frac{\langle\langle \Delta E \rangle\rangle_k(a^{(n)})}{\sigma^2(\Delta E; a^{(n)})}, \quad (26)$$

$$\sigma^2(\Delta E; a) = \langle\langle \Delta E^2 \rangle\rangle_k(a) - \langle\langle \Delta E \rangle\rangle_k^2(a) = -\frac{d}{da} \langle\langle \Delta E \rangle\rangle_k(a).$$

For $a^{(n)}$ sufficiently close to the true value a_k , we can approximate $\sigma^2(\Delta E; a) \approx \delta E^2/12$, and the Newton–Raphson iteration turns into the fixed point iteration:

$$a^{(n+1)} = a^{(n)} + \frac{12}{\delta E^2} \langle\langle \Delta E \rangle\rangle_k(a^{(n)}). \quad (27)$$

Note that the approximation for the action fluctuation σ^2 does not affect the precision of the solution but rather the rate of convergence.⁹¹ In fact, a different choice for $\sigma^2(\Delta E; a)$ was discussed in Ref. 92 to improve the convergence rate. However, the expectation values $\langle\langle \Delta E \rangle\rangle_k$ are not known exactly but only available by means

of Monte Carlo estimators. In practice, after a few iterations, the uncertainty of the $a^{(n)}$ is dominated by the noise of the stochastic estimators for $\langle\langle\Delta E\rangle\rangle_k$. Since the noise from the iteration mixes with the error of the iteration, it is not clear *a priori* that the resulting fluctuations are normal-distributed with a mean around the true solution a_k . This problem, however, has been already solved by Robbins and Monro.⁹³ An under-relaxation of the iteration (27) is essential:

$$a^{(n+1)} = a^{(n)} + c_n \frac{12}{\delta E^2} \langle\langle\Delta E\rangle\rangle_k (a^{(n)}), \quad (28)$$

where the coefficients satisfy $\sum_{n=0}^{\infty} c_n = \infty$ and $\sum_{n=0}^{\infty} c_n^2 < \infty$. It can be shown that if the iteration is truncated at some (large) $n = n_c$, the corresponding values $a^{(n_c)}$ are normal-distributed with the mean coinciding with the true solution a_k .⁹³ This is indeed how we simulate in practice: we generate a variety of potential solutions $a^{(n_c)}$ which are subjected to further calculations of observables the statistical errors of which we obtain by a standard bootstrap analysis.

Let us assume now that we have successfully estimated the log-derivative of the DoS for a variety of different action intervals. Our initial assumption is that the density-of-states is a regular function of the action that can be always approximated in the finite interval $[E_k, E_k + \delta E]$ by a suitable functional expansion. In this case, we find using Taylor's theorem

$$\ln \rho(E) = \ln \rho\left(E_k + \frac{\delta E}{2}\right) + \frac{d \ln \rho}{dE} \Big|_{E=E_k + \delta E/2} \left(E - E_k - \frac{\delta E}{2}\right) + \mathcal{O}(\delta E^2). \quad (29)$$

Thereby, for a given action E , the integer k is chosen such that $E_k \leq E \leq E_k + \delta E$, $E_k = E_0 + k\delta E$. Exponentiating this equation and using (25), it was shown in Ref. 91 that remarkably

$$\rho(E) = \tilde{\rho}(E) \exp\{\mathcal{O}(\delta E^2)\} = \tilde{\rho}(E)[1 + \mathcal{O}(\delta E^2)], \quad (30)$$

$$\tilde{\rho}(E) = \rho_0 \left(\prod_{k=1}^{N-1} e^{a_k \delta E} \right) e^{a_N (E - E_N)}, \quad (31)$$

which we will extensively use below. We will observe that $\rho(E)$ spans many orders of magnitude. The key observation is that our approximation implements *exponential error suppression*, meaning that $\rho(E)$ can be approximated with nearly-constant *relative error* despite it may reach over thousands of orders of magnitude: $1 - \frac{\tilde{\rho}(E)}{\rho(E)} = \mathcal{O}(\delta E^2)$. Finally, some comments are in order: the above LLR formulation uses finite size action intervals, which might raise concerns about ergodicity. In practice we have studied \mathbb{Z}_3 , $U(1)$, $SU(2)$ and $SU(3)$ gauge theories and have never encountered any ergodicity problem. We also point out that the ergodicity properties can be easily improved by using the *replica exchange* method, where one uses overlapping action intervals and exchanges configurations of neighboring intervals with the corresponding exchange probability (see Ref. 91 for details).

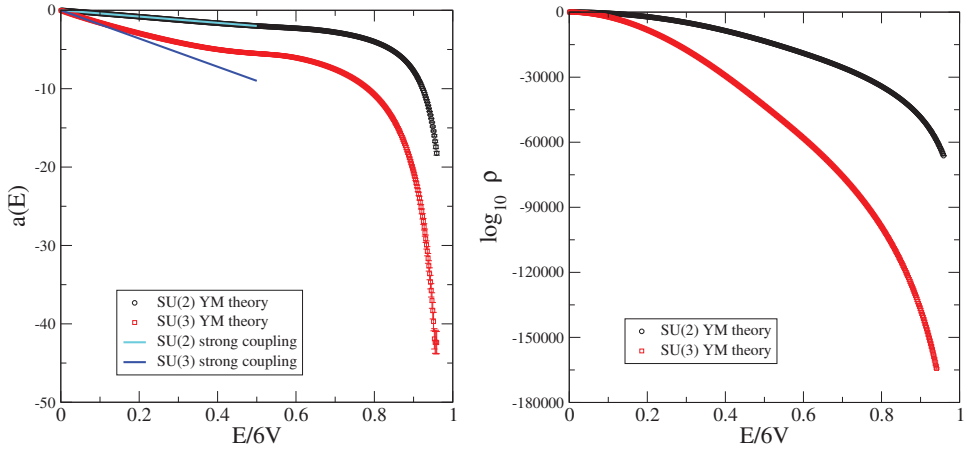


Fig. 1. Left: The LLR coefficient a as a function of the action E in units of its maximal value $6V$, $V = 10^4$ is the 4d lattice volume. Right: the corresponding density-of-states $\rho(E)$.

3.2. The $SU(2)$ and $SU(3)$ showcase

Let us now specialize to the case of $SU(N_c)$, $N_c = 2, 3$ gauge theory. The dynamical degrees of freedom are the link variables $U_\mu(x) \in SU(N_c)$. We will use the Wilson action and show results for 10^4 lattices. For each action interval, we used 200 Newton–Raphson steps for thermalization and 600 Robbins–Monro under-relaxation steps. We generated 20 independent candidates for the corresponding LLR coefficient a , which is subsequently used in a bootstrap error analysis. The numerical findings shown here complement our earlier results in Ref. 90. Our findings for the LLR coefficients for a $SU(2)$ and a $SU(3)$ theory are shown in Fig. 1.

The probabilistic density generating a lattice configuration within the action interval $[E, E + dE]$ consists of an entropy factor, i.e. the density of states, and the Gibbs factor: $P(E) = \rho(E) \exp(\beta E)$. Because E is an extensive quantity, $P(E)$ possesses a sharp maximum (or several of them in case the theory has a first order phase transition⁹¹). The position of the extremal points can be found by

$$\frac{dP}{dE} = P(E) \left[\frac{d \ln \rho}{dE} + \beta \right] = P(E) [a(E) + \beta] = 0. \quad (32)$$

If the LLR coefficients $a(E)$ are monotonic as a function of E , $P(E)$ has a single maximum for all β and does not have a first order phase transition (for the given aspect ratio of spatial and timelike lattice size for the simulation). For small β , the action, i.e. the plaquette expectation value can be calculated using Taylor-expansion with respect to β — the so-called strong coupling expansion:

$$\langle S[U] \rangle = s_0 \beta + \mathcal{O}(\beta^2), \quad s_0 = \frac{1}{4} \text{ for } SU(2), \quad s_0 = \frac{1}{18} \text{ for } SU(3). \quad (33)$$

For small β only coefficients $a(E)$ close to zero are relevant in the large volume limit because of (32). Here we approximate to leading order

$$a(E) = a_0 E + \mathcal{O}(E^2), \quad \rho(E) = \rho_0 \exp\left(\frac{a_0}{2} E^2 + \mathcal{O}(E^3)\right).$$

With this density-of-states, the action expectation value becomes

$$\langle S[U] \rangle = \frac{\int dE \rho(E) \exp(\beta E) E}{\int dE \rho(E) \exp(\beta E)} = -\frac{\beta}{a_0}.$$

Comparing this with the strong coupling result in (33), we find at small E that

$$a(E) = -4E + \mathcal{O}(E^2) \quad \text{for SU(2)}, \quad a(E) = -18E + \mathcal{O}(E^2) \quad \text{for SU(3)}. \quad (34)$$

The leading order for $a(E)$ at small values for E is also shown in Fig. 1. Once the coefficients $a(E)$ are known, the density-of-states $\rho(E)$ can be estimated with the help of (30). For each action interval $[E, E + \delta E]$, we have generated 20 independent candidates for $a(E)$ after 800 Robbins–Monro iterations. The density and its error are then obtained by a standard bootstrap analysis. The result is also shown in Fig. 1 (right panel). Note the logarithmic scale (base 10). By virtue of the exponential error suppression, we can calculate the density-of-states over more than 10^6 orders of magnitude with good relative error.

3.3. The LLR method for theories with a sign problem

The density-of-states method can be generalized to calculate high precision observables other than those depending on the action. For example in Ref. 94, the probability distribution of the Polyakov line was calculated with extreme precision for a study of 2-color QCD at finite densities of heavy quarks. Here we focus on a generalization of the LLR method that will allow us to simulate theories with a sign problem.

The partition sum of such a theory and its *phase-quenched* counterpart are

$$Z(\mu) = \int \mathcal{D}\phi e^{S_R[\Phi](\mu)} \exp(iS_I[\phi](\mu)), \quad Z_{\text{mod}}(\mu) = \int \mathcal{D}\phi e^{S_R[\Phi](\mu)}, \quad (35)$$

where μ is the chemical potential. With the help of the phase factor expectation value $Q(\mu)$, we trivially cast (35) into

$$Z(\mu) = Q(\mu) Z_{\text{mod}}(\mu), \quad Q(\mu) = \frac{Z(\mu)}{Z_{\text{mod}}(\mu)} = \langle \exp(iS_I[\phi](\mu)) \rangle_{\text{mod}}. \quad (36)$$

Since observables of the phase-quenched theory are accessible with standard Monte Carlo simulations, this implies that the solution of the sign problem is relegated to the calculation of $Q(\mu)$. The LLR approach to calculate $Q(\mu)$ starts with the definition of the density-of-states for the imaginary part of the action:⁹⁵

$$\rho(s) = N \int \mathcal{D}\phi \delta(s - S_I[\phi](\mu)) e^{S_R[\Phi](\mu)}, \quad Q(\mu) = \frac{\int ds \rho(s) \exp(is)}{\int ds \rho(s)}. \quad (37)$$

Such a generalized density-of-states was first introduced by Gocksch⁹⁶ to address the phase factor of the quark determinant of finite density QCD, or for studies of the theta angle dependence in spin systems in Refs. 97 and 98. The theoretical framework of the LLR method as discussed in Subsec. 3.1 can be transferred to the case (37): the intervals now discretize the imaginary part of the action S_I , and after the estimate of the LLR coefficients a_k , the probability distribution $\rho(s)$ can be retrieved.

3.4. The \mathbb{Z}_3 theory at finite densities

For a first showcase, we briefly review the LLR approach to the \mathbb{Z}_3 spin model at finite chemical potential μ .⁹⁵ The degrees of freedom $\phi(x) \in \{1, z, z^*\}$, $z = (1 + i\sqrt{3})/2$ are associated with the N^3 sites of the three-dimensional lattice. The partition function and the action of the system are given by

$$Z(\mu) = \sum_{\{\phi\}} \exp(S[\phi]), \quad S[\phi] = \tau \sum_{x,\nu} \phi_x \phi_{x+\nu}^* + \sum_x (\eta \phi_x + \bar{\eta} \phi_x^*), \quad (38)$$

with $\eta = \kappa e^\mu$ and $\bar{\eta} = \kappa e^{-\mu}$. This theory has a real dual formulation,^{34,35,41} and can be efficiently simulated with the flux algorithm.²⁰ It is therefore ideally suited for testing the LLR approach (for a simulation with the related density-of-states FFA (functional fit approach) see Refs. 92, 99, 100). We introduce

$$N_0 = \sum_x \delta(\phi(x), 1), \quad N_z = \sum_x \delta(\phi(x), z), \quad N_{z^*} = \sum_x \delta(\phi(x), z^*), \quad (39)$$

which correspond to the total number of a particular center element of the configuration. It turns out that the imaginary part of the action is proportional to the *center imbalance* $\Delta N := N_z - N_{z^*}$ on the lattice. Hence, the LLR method targets the probability distribution of this quantity, and we introduce the generalized density

$$\rho(n) := \sum_{\{\phi\}} \delta(n, \Delta N[\phi]) \exp(S[\phi] + \kappa(3N_0[\phi] - V) \cosh(\mu)). \quad (40)$$

The histogram method generates configurations with the Gibbs factor given by the exponential in (40) and keeps track of $\Delta N[\phi]$ of each configuration. The result for a 24^3 lattice, $\tau = 0.17$ and $\kappa = 0.01$ is shown in Fig. 2. The histogram method is riddled by an *overlap problem*: configurations with high ΔN are hardly generated leading to large relative uncertainties. The LLR method does solve this problem due to its inherent exponential error suppression: the density-of-states is obtained with nearly constant relative errors over 70 orders of magnitude. With the density-of-states at hand, the partition function can be written as a simple sum: $Z(\mu) = \sum_n \rho(n) \cos(\sqrt{3}\kappa \sinh(\mu)n)$. Although we have reached a very good (relative) precision for ρ , a new challenge arises from the oscillating sum, which, by virtue of cancellations, results in an exponentially small result

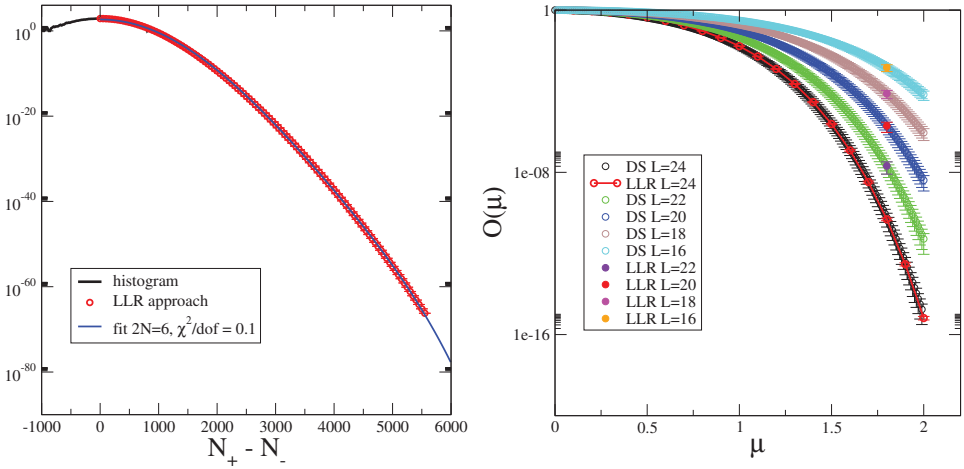


Fig. 2. (Color online) Left: The probability distribution of the center imbalance ΔN for the \mathbb{Z}_3 theory on a 24^3 lattice with $\tau = 0.17$ and $\kappa = 0.01$. Also shown (red symbols) is the result from the LLR approach. Right: The overlap factor as a function of μ ; LLR results in comparison to the known results from the dual theory (figure from Ref. 95).

(see (9)). Standard interpolation schemes use a piecewise interpolation of the discrete set of points and seek convergence by decreasing the spacing δE . It became clear very early on that this approach lacks the precision to obtain this signal. We are therefore using an iterative refinement of the approximation in functional space: $\ln \rho(n) = \lim_{N \rightarrow \infty} \sum_{k=1}^N c_k f_k(n)$, where $f_k(n)$ are basis functions. The approximation arises from the truncation of the above sum. For the \mathbb{Z}_3 spin system, good results are obtained by using powers of n : $f_k(n) = n^{2k}$. Here we have exploited the symmetry $\rho(-n) = \rho(n)$, which eliminates odd powers of n from the basis. Figure 2, left panel, shows the method at work: a truncation at $N = 3$ already leaves us with a good representation of the data at the level of $\chi^2/\text{dof.} = 0.1$. Once a good functional representation of the data is obtained, the sums for the overlap factor,

$$Q(\mu) = \frac{\sum_n \rho(n) \cos(\sqrt{3}\kappa \sinh(\mu)n)}{\sum_n \rho(n)},$$

can be obtained in a (semi-)analytical way. Figure 2, right panel, shows the result for the overlap factor for several values of μ .⁹⁵ We find a very good agreement with the known results from the simulations of the dual real theory.

Acknowledgments

We thank F. Bruckmann, B. Lucini, T. Sulejmanpasic, and A. Rago for discussions. K. Langfeld is supported by the Leverhulme Trust (grant RPG-2014-118) and STFC (grant ST/L000350/1). C. Gattringer is supported by DFG TRR55, and FWF grant I 1452-N27.

References

1. S. Borsanyi, *PoS LATTICE2015*, 015 (2016), arXiv:1511.06541.
2. D. Sexty, *PoS LATTICE2014*, 016 (2014), arXiv:1410.8813.
3. C. Gattringer, *PoS LATTICE2013*, 002 (2014), arXiv:1401.7788.
4. G. Aarts, *PoS LATTICE2012*, 017 (2012), arXiv:1302.3028.
5. U. Wolff, *PoS LATTICE2010*, 020 (2010), arXiv:1009.0657.
6. P. de Forcrand, *PoS LAT2009*, 010 (2009), arXiv:1005.0539.
7. S. Chandrasekharan, *PoS LATTICE2008*, 003 (2008), arXiv:0810.2419.
8. C. Schubert, *Phys. Rep.* **355**, 73 (2001).
9. H. Gies and K. Langfeld, *Nucl. Phys. B* **613**, 353 (2001).
10. K. Langfeld, L. Moyaerts and H. Gies, *Nucl. Phys. B* **646**, 158 (2002).
11. H. Gies, K. Langfeld and L. Moyaerts, *J. High Energy Phys.* **06**, 018 (2003).
12. M. Troyer and U.-J. Wiese, *Phys. Rev. Lett.* **94**, 170201 (2005).
13. C. Gattringer and T. Kloiber, *Nucl. Phys. B* **869**, 56 (2013).
14. C. Gattringer and T. Kloiber, *Phys. Lett. B* **720**, 210 (2013).
15. T. Korzec, I. Vierhaus and U. Wolff, *Comput. Phys. Commun.* **182**, 1477 (2011).
16. T. Rindlisbacher and P. de Forcrand, arXiv:1602.09017.
17. N. Prokof'ev and B. Svistunov, *Phys. Rev. Lett.* **87**, 160601 (2001).
18. U. Wolff, *Nucl. Phys. B* **810**, 491 (2009).
19. Y. D. Mercado and C. Gattringer, *Nucl. Phys. B* **862**, 737 (2012).
20. Y. D. Mercado, H. G. Evertz and C. Gattringer, *Comput. Phys. Commun.* **183**, 1920 (2012).
21. D. Banerjee and S. Chandrasekharan, *Phys. Rev. D* **81**, 125007 (2010).
22. U. Wolff, *Phys. Rev. D* **79**, 105002 (2009).
23. P. Weisz and U. Wolff, *Nucl. Phys. B* **846**, 316 (2011).
24. M. Hogervorst and U. Wolff, *Nucl. Phys. B* **855**, 885 (2012).
25. J. Siefert and U. Wolff, *Phys. Lett. B* **733**, 11 (2014).
26. M. G. Endres, *PoS LAT2006*, 133 (2006), arXiv:hep-lat/0609037.
27. M. G. Endres, *Phys. Rev. D* **75**, 065012 (2007).
28. U. Wolff, *Nucl. Phys. B* **824**, 254 (2010) [Erratum: *ibid.* **834**, 395 (2010)].
29. F. Bruckmann, C. Gattringer, T. Kloiber and T. Sulejmanpasic, *Phys. Lett. B* **749**, 495 (2015) [Erratum: *ibid.* **751**, 595 (2015)].
30. F. Bruckmann, C. Gattringer, T. Kloiber and T. Sulejmanpasic, *Phys. Rev. Lett.* **115**, 231601 (2015).
31. F. Bruckmann, C. Gattringer, T. Kloiber and T. Sulejmanpasic, *PoS LATTICE2015*, 210 (2016), arXiv:1512.05482.
32. U. Wolff, *Nucl. Phys. B* **832**, 520 (2010).
33. T. Rindlisbacher and P. Forcrand, *PoS LATTICE2014* (2015), arXiv:1512.05684.
34. A. Patel, *Nucl. Phys. B* **243**, 411 (1984).
35. T. A. DeGrand and C. E. DeTar, *Nucl. Phys. B* **225**, 590 (1983).
36. F. Karsch and H. Wyld, *Phys. Rev. Lett.* **55**, 2242 (1985).
37. G. Bergner, J. Langelage and O. Philipsen, *J. High Energy Phys.* **03**, 039 (2014).
38. J. Langelage, M. Neuman and O. Philipsen, *J. High Energy Phys.* **09**, 131 (2014).
39. J. Glesaaen, M. Neuman and O. Philipsen, arXiv:1512.05195.
40. G. Bergner, J. Langelage and O. Philipsen, *J. High Energy Phys.* **11**, 010 (2015).
41. Y. D. Mercado, H. G. Evertz and C. Gattringer, *Phys. Rev. Lett.* **106**, 222001 (2011).
42. C. Gattringer, *Nucl. Phys. B* **850**, 242 (2011).
43. Y. D. Mercado, C. Gattringer and A. Schmidt, *Phys. Rev. Lett.* **111**, 141601 (2013).
44. M. Panero, *J. High Energy Phys.* **05**, 066 (2005).
45. T. Korzec and U. Wolff, *PoS LATTICE2010*, 029 (2010), arXiv:1011.1359.

46. T. Korzec and U. Wolff, *Nucl. Phys. B* **871**, 145 (2013).
47. M. Caselle, M. Panero, R. Pellegrini and D. Vadacchino, *J. High Energy Phys.* **01**, 105 (2015).
48. M. Caselle, M. Panero and D. Vadacchino, *J. High Energy Phys.* **02**, 180 (2016).
49. C. Gattringer, T. Kloiber and V. Sazonov, *Nucl. Phys. B* **897**, 732 (2015).
50. C. Gattringer, T. Kloiber and M. Müller-Preussker, *Phys. Rev. D* **92**, 114508 (2015).
51. T. Kloiber and C. Gattringer, *PoS LATTICE2014*, 345 (2014).
52. A. Schmidt, P. de Forcrand and C. Gattringer, *PoS LATTICE2014*, 209 (2015).
53. C. Gattringer and A. Schmidt, *Phys. Rev. D* **86**, 094506 (2012).
54. Y. D. Mercado, C. Gattringer and A. Schmidt, *Comput. Phys. Comun.* **184**, 1535 (2013).
55. P. Rossi and U. Wolff, *Nucl. Phys. B* **248**, 105 (1984).
56. F. Karsch and K. H. Mütter, *Nucl. Phys. B* **313**, 541 (1989).
57. N. D. Hari Dass, *Nucl. Phys. B (Proc. Suppl.)* **94**, 665 (2001).
58. N. D. Hari Dass and D.-S. Shin, *Nucl. Phys. B (Proc. Suppl.)* **94**, 670 (2001).
59. N. D. Hari Dass, *Nucl. Phys. B (Proc. Suppl.)* **83**, 950 (2000).
60. J. W. Cherrington, D. Christensen and I. Khavkine, *Phys. Rev. D* **76**, 094503 (2007).
61. J. W. Cherrington, *Nucl. Phys. B* **794**, 195 (2008).
62. J. W. Cherrington and J. D. Christensen, *Nucl. Phys. B* **813**, 370 (2009).
63. J. W. Cherrington, *Nucl. Phys. B* **835**, 29 (2010).
64. J. W. Cherrington, *Nucl. Phys. B* **835**, 51 (2010).
65. P. de Forcrand and M. Fromm, *Phys. Rev. Lett.* **104**, 112005 (2010).
66. W. Unger and P. de Forcrand, *J. Phys.* **G38**, 124190 (2011).
67. P. de Forcrand *et al.*, *Phys. Rev. Lett.* **113**, 152002 (2014).
68. M. Salmhofer, *Nucl. Phys. B* **362**, 641 (1991).
69. D. J. Cecile and S. Chandrasekharan, *Phys. Rev. D* **77**, 014506 (2008).
70. S. Chandrasekharan, *Phys. Lett. B* **536**, 72 (2002).
71. R. De Pietri, A. Feo, E. Seiler and I.-O. Stamatescu, *Phys. Rev. D* **76**, 114501 (2007).
72. T. Rindlisbacher and P. de Forcrand, *J. High Energy Phys.* **02**, 051 (2016).
73. I. O. Stamatescu, *Phys. Rev. D* **25**, 1130 (1982).
74. C. Gattringer and V. Sazonov, *Phys. Rev. D* **93**, 034505 (2016).
75. M. Kniely and C. Gattringer, *PoS LATTICE2014*, 206 (2015), arXiv:1502.00788.
76. C. Gattringer, *Nucl. Phys. B* **559**, 539 (1999).
77. C. Gattringer, *Nucl. Phys. B* **543**, 533 (1999).
78. C. Gattringer, *Int. J. Mod. Phys. A* **14**, 4853 (1999).
79. U. Wolff, *Nucl. Phys. B* **814**, 549 (2009).
80. D. J. Cecile and S. Chandrasekharan, *Phys. Rev. D* **77**, 054502 (2008).
81. M. G. Endres, *Phys. Rev. A* **85**, 063624 (2012).
82. S. Chandrasekharan, *Phys. Rev. D* **82**, 025007 (2010).
83. S. Chandrasekharan and A. Li, *Phys. Rev. Lett.* **108**, 140404 (2012).
84. S. Chandrasekharan and A. Li, *Phys. Rev. D* **85**, 091502 (2012).
85. S. Chandrasekharan, *Phys. Rev. D* **86**, 021701 (2012).
86. F. Wang and D. P. Landau, *Phys. Rev. Lett.* **86**, 2050 (2001).
87. J. Xu and H.-R. Ma, *Phys. Rev. E* **75**, 041115 (2007).
88. S. Sinha and S. Kumar Roy, *Phys. Lett. A* **373**, 308 (2009).
89. B. Berg and T. Neuhaus, *Phys. Rev. Lett.* **68**, 9 (1992).
90. K. Langfeld, B. Lucini and A. Rago, *Phys. Rev. Lett.* **109**, 111601 (2012).
91. K. Langfeld, B. Lucini, R. Pellegrini and A. Rago, arXiv:1509.08391.
92. C. Gattringer and P. Törek, *Phys. Lett. B* **747**, 545 (2015).
93. H. Robbins and S. Monro, *Ann. Math. Stat.* **22**, 400 (1951).

94. K. Langfeld and J. M. Pawłowski, *Phys. Rev. D* **88**, 071502 (2013).
95. K. Langfeld and B. Lucini, *Phys. Rev. D* **90**, 094502 (2014).
96. A. Gocksch, *Phys. Rev. Lett.* **61**, 2054 (1988).
97. V. Azcoiti *et al.*, *Nucl. Phys. B (Proc. Suppl.)* **119**, 1009 (2003).
98. V. Azcoiti, E. Follana and A. Vaquero, *Nucl. Phys. B* **851**, 420 (2011).
99. Y. Delgado Mercado, P. Törek and C. Gattringer, *PoS LATTICE2014*, 203 (2015).
100. C. Gattringer *et al.*, *PoS LATTICE2015*, 194 (2015), arXiv:1511.07176.